

# Multitechnique Characterization of Fatty Acid-Modified Microgels

Mary L. Kraft and Jeffrey S. Moore\*

The Beckman Institute for Advanced Science and Technology,  
The University of Illinois at Urbana-Champaign, Urbana, Illinois 61801

Received August 30, 2003. In Final Form: December 9, 2003

The structure of fatty acid-modified hydrogel objects ( $\mu$ gels) created within microfluidic devices for controlled-release or sensory applications was characterized by various imaging and spectroscopic methods. Imaging with scanning electron microscopy revealed that the surface was rough and irregular on the micrometer scale. Examination of planar model systems analogous to the modified  $\mu$ gels with X-ray photoelectron spectroscopy and secondary ion mass spectroscopy showed that a fatty acid coating formed when the reaction conditions were conducive to covalent-bond formation. Visualization of the selectively stained lipophilic coating with laser scanning confocal microscopy while the  $\mu$ gel was positioned within a microfluidic channel demonstrated that the coating was confined to the  $\mu$ gel's periphery. Finally, using transmission electron microscopy, the thickness of the region functionalized with fatty acids was determined to be around  $9\ \mu\text{m}$  on samples very similar to those integrated into microfluidic devices. By using transmission electron microscopy to monitor the thickness of the fatty acid coating produced with different reaction conditions, it may be possible to customize these hybrid materials for specific sensory or controlled-release applications.

## Introduction

Microscale compartmentalization is a fundamental characteristic of life. Bilayer membranes regulate the passage of materials into and out of each cell and organelle.<sup>1</sup> To study transport and other crucial processes mediated by biomembranes, synthetic lipid bilayers supported on hydrophilic polymer cushions have been extensively employed as simplified model systems.<sup>2</sup> These synthetic, supported membranes provide a cell-like environment for the incorporation of transmembrane proteins, and like biological membranes, the selectively permeable lipid bilayers are capable of maintaining a chemical gradient that might be utilized to generate energy.<sup>3</sup>

The ability to separate chemically distinct environments has inspired the creation of microcompartments based on lipid and hydrogel hybrids for controlled-release or sensory applications.<sup>4–11</sup> Gao and Huang reported the preparation of solid core liposomes, made by encapsulating agarose-gelatin particles within lipid vesicles.<sup>4</sup> Pennefather and co-workers improved the stability of similar hybrids by covalently attaching fatty acids or lipids to the surface of a hydrogel core, which templated the subsequent self-assembly of a lipid bilayer around the exterior.<sup>5,6</sup> The

hydrogel–lipid conjugates, or Lipobeads, were able to sustain a calcium gradient across the lipid bilayer that could be abolished by the introduction of an ionophore.<sup>6</sup> Needham and co-workers exploited the formation of such an ion gradient for the triggered release of materials entrapped within hydrogel microspheres coated with lipid bilayers.<sup>7,8</sup> The pH-sensitive hydrogel microspheres were loaded with the drug doxorubicin, compacted by exposure to a buffered solution of a reduced pH, and coated with a lipid bilayer. Because lipid bilayers are essentially impermeable to charged species, the lipid-coated hydrogel cores remained in the compact state when bathed by an elevated pH buffer solution that otherwise swells uncoated hydrogels. Poration of the lipid bilayer by an electrical pulse allowed the external buffer ions to enter the hydrogel microcompartment, triggering expansion of the object through ionization of the pH-sensitive hydrogel network, and, consequently, releasing the entrapped doxorubicin.

For sensory applications, a simple method to incorporate lipid-coated environmentally sensitive hydrogels within microfluidic devices would be highly advantageous. With this intent, we previously combined the approaches of Pennefather et al. and Needham et al. to covalently attach a coating of lipophilic fatty acids to the periphery of pH-sensitive hydrogel objects ( $\mu$ gels) within microfluidic channels using an in situ process (Figure 1).<sup>9–11</sup> Like a lipid bilayer, the fatty acid coating prevented the influx of buffer ions into the pH-sensitive  $\mu$ gel, thereby establishing a chemical gradient that allowed the  $\mu$ gel to remain compact while bathed in a buffered solution of elevated pH that otherwise elicits the expansion of unmodified samples. Permeability of the fatty acid coating to ions could be chemically induced with buffered surfactant solutions, initiating complete expansion of the  $\mu$ gel through an asymmetric process.<sup>9</sup>

Knowledge of the coating thickness is crucial for the optimization of these objects for sensory applications, but very little is known about the structure of the modified  $\mu$ gels. Visual assessment of the  $\mu$ gel morphology performed with scanning electron microscopy (SEM) revealed a

\* To whom correspondence should be addressed. Phone: (217) 244-4024. E-mail: moore@scs.uiuc.edu.

(1) Voet, D.; Voet, J. G. *Biochemistry*, 2nd ed.; John Wiley & Sons: New York, 1995.

(2) Sackmann, E.; Tanaka, M. *Trends Biotechnol.* **2000**, *18*, 58–64.

(3) Sackmann, E. *Science* **1996**, *271*, 43–48.

(4) Gao, K.; Huang, L. *Biochim. Biophys. Acta* **1987**, *897*, 377–383.

(5) Ng, C. C.; Cheng, Y.-L.; Pennefather, P. S. *Macromolecules* **2001**, *34*, 5759–5765.

(6) Jin, T.; Pennefather, P.; Lee, P. I. *FEBS Lett.* **1996**, *397*, 70–74.

(7) Kiser, P. F.; Wilson, G.; Needham, D. *Nature* **1998**, *394*, 459–462.

(8) Kiser, P. F.; Wilson, G.; Needham, D. *J. Controlled Release* **2000**, *68*, 9–22.

(9) Kraft, M. L.; Moore, J. S. *J. Am. Chem. Soc.* **2001**, *123*, 12921–12922.

(10) Kraft, M. L.; Moore, J. S. *Langmuir* **2003**, *19*, 910–915.

(11) Beebe, D. J.; Moore, J. S.; Yu, Q.; Liu, R. H.; Kraft, M. L.; Jo, B.; Devadoss, C. *Proc. Natl. Acad. Sci. U.S.A.* **2000**, *97*, 13488–13493.

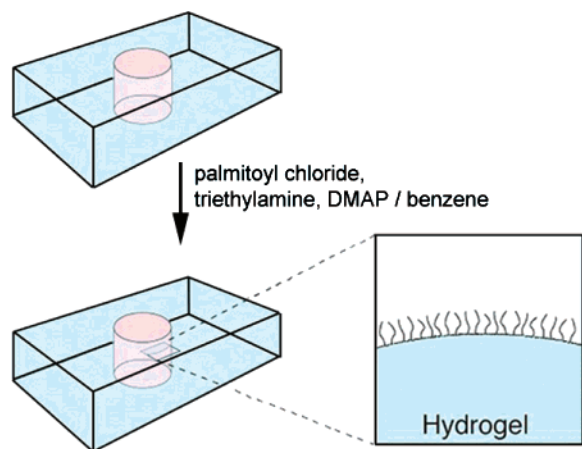


**Figure 1.** The fatty acid coating is created by reacting the hydroxy-terminated hydrogel object with lipophilic acid chlorides.

jagged and irregular  $\mu$ gel surface, and indicating the structural assessment of the fatty acid-coated  $\mu$ gels would be challenging because many surface characterization techniques require smooth substrates for the acquisition of depth profiles. To overcome this obstacle, we developed a planar model system and modified  $\mu$ gels that were amenable to investigation with traditional surface characterization and microscopy techniques, as will be described in this paper. The presence of the fatty acid coating was verified through the examination of planar model systems with X-ray photoelectron spectroscopy (XPS) and secondary ion mass spectrometry (SIMS). Laser scanning confocal microscopy (LSCM) and the use of a lipophilic fluorescent dye confirmed the coating was mainly confined to the periphery of the modified  $\mu$ gel. Last, the thickness of the  $\mu$ gel's perimeter functionalized with fatty acids was determined by imaging modified  $\mu$ gels with transmission electron microscopy (TEM).

### Experimental Section

**Materials.** To remove the polymerization inhibitor packaged with the monomers for transport, acrylic acid (AA, Fisher Scientific) and 2-hydroxyethyl methacrylate (HEMA, Aldrich) were each vacuum-distilled in the presence of the polymerization inhibitor 4-methoxyquinone prior to use. Poly(2-hydroxyethyl methacrylate) (pHEMA, MW ca. 20 000, Aldrich), 2,2'-dimethoxy-2-phenylacetophenone (DMPA, Aldrich), ethylene glycol dimethacrylate (EGDMA, Aldrich), 3-(trimethoxysilyl)propyl methacrylate (MSPMA, Aldrich), 16-hydroxyhexadecanoic acid (Aldrich), (diethylamino)sulfur trifluoride (DAST, Aldrich), oxalyl chloride (Aldrich), palmitoyl chloride (Aldrich), oleoyl chloride (Aldrich), 4-(dimethylamino)pyridine (DMAP, Aldrich), triethylamine (NET<sub>3</sub>, Fisher), the gold colloid solution (20-nm diameter, Sigma), osmium tetroxide (4% aqueous, Polysciences), and 1,1'-dioctadecyl-3,3,3',3'-tetramethylindolodicarbocyanine perchlorate (DiD, Molecular Probes) were all used as received without further purification. All solvents were used without further purification unless otherwise indicated. For microchannel fabrication, glass microscope slides (75 × 50 × 1 mm) and glass coverslips (22 × 50 mm, no. 1 thickness, 180- $\mu$ m thick) were obtained from Fisher Scientific, and UV-curable adhesive (Norland Optical Adhesive no. 61) from Norland Products (New Brunswick, NJ). Surface modifications were performed with a Harvard Apparatus PHD 2000 remote control with 6/10 multitrack programmable syringe pump, which allowed the modification of up to six  $\mu$ gels at a time. For the preparation of planar hydrogel substrates, single-side polished, reclaimed silicon wafers (3-in. diameter) were obtained from Montco Silicon Technologies, Inc., and the Teflon FEP fluoropolymer film was purchased from American Durafilm Co., Inc. To embed the  $\mu$ gels for TEM, an Araldite 502 kit was purchased from Electron Microscopy Sciences and prepared

according to the manufacturer's specifications. Gilder thin bar electron microscopy grids (nickel, 400 mesh) were purchased from Electron Microscopy Sciences.

**Preparation and Characterization of pH-Sensitive  $\mu$ gels within Microfluidic Channels.** The photolithographic patterning of hydrogels within microfluidic devices was performed by previously reported procedures.<sup>9,11,12</sup> A brief account is given in the following.

**Fabrication of Microchannels.** Channels were made by affixing two glass coverslips (22 × 50 mm, 180- $\mu$ m thick) to a glass microscope slide (75 × 50 × 1 mm) with UV-curable glue (Norland Optical Adhesive no. 61) such that the coverslips were oriented parallel to each other but separated by approximately 2 mm. The glue was cured for 5 min with a Kinsten Exposure Unit (KVB-30, Computronic Corp., Ltd., Australia). A third coverslip was cured so that it covered the separation, forming the top of an approximately 180- $\mu$ m-deep channel. After curing the adhesive, plastic pipet tips were attached to both ends of the channel with DURO Quick Set epoxy resin to serve as the inlet and outlet.

**Photopolymerization of pH-Sensitive  $\mu$ gels.** pH-sensitive  $\mu$ gels were made from a monomer mixture of 4:1 mol HEMA/AA with 1 wt % EGDMA, and 3 wt % DMPA. The mixture was injected into the channel and placed on the stage of an Olympus Epi-Fluorescent microscope (BX-60). A photomask of a 400- $\mu$ m diameter circle made of transparency film printed on a high-resolution printer (5080 dpi, Linotype Herkules Imagesetter, Heidelberg, Germany) was positioned on top of the channel. Photopolymerization was carried out by 2-min of exposure of the unmasked region to UV light from a high-pressure mercury lamp that was filtered through a near-UV filter cube (360–370-nm band-pass, U-MNUA, type BP360–370) and intensified with the 2× lens. After polymerization, the channel was flushed with methanol and acetone and dried under a nitrogen stream.

**Surface Modification of pH-Sensitive  $\mu$ gels with Palmitoyl Chloride.** A 50-mL syringe fitted with a 16-gauge needle was charged with 0.1 M palmitoyl chloride, 0.1 M NET<sub>3</sub>, and 0.01 M DMAP in benzene. Silicone tubing (1.58-mm i.d., 2.41-mm o.d., HelixMark) was used to connect the needle to the inlet of a channel that contained a  $\mu$ gel and the outlet to a waste container. Using a Harvard Apparatus PHD Programmable syringe pump, the solution was flowed through the channel at a rate of 200 mL/h until the solution filled the channel, then the pump was reprogrammed to a rate of 5 mL/h. After approximately half of the modification solution was consumed (~4.5 h), the channels were flushed with methylene chloride to remove precipitate, the needles and tubing were replaced, and the pump was restarted so the remainder of the solution flowed through the channel in the direction opposite to that previously employed. Upon completion, the channels were flushed with methylene chloride to remove unreacted reagents and dried under a nitrogen stream.

**SEM.** SEM imaging was performed on modified and unmodified  $\mu$ gels that were dried with a nitrogen stream. The samples were carefully removed from the channels so that only a small piece of glass remained attached to the bottom of each  $\mu$ gel. Using a gold/palladium target, a conductive metal coating (~25-nm thick) was deposited on each  $\mu$ gel using a Denton Desk II TSC turbo-pumped sputter coater. Imaging was performed on a Phillips XL30 ESEM-FEG equipped with an Everhart-Thornley secondary electron detector using an accelerating voltage of 5 kV.

**LSCM.** To selectively stain the fatty acid coating, a solution of the lipophilic, fluorescent dye DiD in methylene chloride (5 mg/mL) was introduced to the channel containing the  $\mu$ gel of interest. After a 5-min incubation at room temperature, the channel was manually rinsed with methylene chloride (5 mL) to remove excess dye and dried under a nitrogen stream. The channel was filled with water and the hydrated  $\mu$ gel was imaged with a Leica TCS SP2 LSCM using a 20× objective, beam expander 6, and a pinhole of a 1.01 airy disk. The HeNe 633-nm laser (49% power setting) was used for the excitation source, and the emission was monitored from 650 to 670 nm with a photomultiplier tube (PMT). Both modified and unmodified

(negative control)  $\mu$ gels were stained and imaged under these conditions.

**Preparation and Characterization of Fatty Acid-Modified Planar Hydrogels.** The procedure for the photolithographic patterning of hydrogels on planar substrates was derived from previously reported procedures,<sup>13–17</sup> as described in the following.

**Surface Treatment of Silicon Wafers.** Silicon wafers were cleaned in an oxygen plasma at a power of 70 W for 2 min (March PLASMOD system). To modify the wafer surface with acrylate functionalities, the wafers were placed in a 65 °C solution of MSPMA in toluene (1:9 vol) with trace water (1 drop) for 20 min with occasional gentle swirling. The wafers were removed from the solution, washed with 2-propanol, methanol, and acetone, and dried under a nitrogen stream.

**Preparation of Planar Hydrogel Substrates.** The prepolymer mixture was composed of a HEMA component (pHEMA and HEMA at 1:3 w/w) and AA (4:1 monomer units) with EGDMA (1 vol %) and DMPA (3 wt %). The prepolymer mixture was stirred overnight at room temperature and filtered through a coarse-frit funnel to remove insoluble particles. The prepolymer mixture was spin-coated onto the acrylate-functionalized wafers for 10 s at 500 rpm followed by 30 s at 1000 rpm, and a piece of Teflon FEP fluoropolymer film was carefully positioned over the prepolymer-coated wafer. A photomask of  $1 \times 1$  cm<sup>2</sup> squares, made on a high-resolution printer (5080 dpi, Linotype Herkules Imagesetter, Heidelberg, Germany), was positioned over the wafer, and the unmasked regions were polymerized by exposure (3 min) to a high-pressure mercury lamp (350 W, Kasper Contact Aligner). The Teflon film was removed, and the wafer was rinsed with methanol, water, and acetone to remove unpolymerized prepolymer mixture and dried in air. The wafers were diced so that each piece was patterned with a  $1 \times 1$  cm<sup>2</sup> hydrogel substrate approximately 20- $\mu$ m thick.

**Synthesis of Fluorinated Fatty Acid Chlorides (Representative Procedure).** Each of these reactions was performed several times, and the optimized procedure is given below. <sup>1</sup>H NMR and <sup>13</sup>C NMR spectra were recorded at an NMR spectrometer frequency of 400 or 500 MHz. Elemental analysis was performed by the University of Illinois Micro Analytical Service Laboratory. Low-resolution electron ionization mass spectra were obtained on a 70-VSE-B spectrometer operating at 70 eV.

**Methyl 16-Hydroxyhexadecanoate.** Concentrated H<sub>2</sub>SO<sub>4</sub> (36 drops) was added to a solution of 16-hydroxyhexadecanoic acid (5.098 g,  $1.871 \times 10^{-2}$  mol) in methanol (200 mL). The solution was refluxed overnight (13.5 h). After cooling, the solution was transferred to a separatory funnel, and then water (140 mL) and ether (600 mL) were added. The layers were separated; the organic layer was washed with water ( $3 \times 100$  mL), saturated NaHCO<sub>3</sub>(aq) ( $1 \times 100$  mL), and brine ( $1 \times 100$  mL). The organic layer was dried over MgSO<sub>4</sub> and concentrated via rotary evaporation yielding 5.30 g (99%) of methyl 16-hydroxyhexadecanoate as a white solid. Mp 54.5–56 °C. <sup>1</sup>H NMR (CDCl<sub>3</sub>):  $\delta$  3.657 (s, 3H), 3.629 (t, 6.66 Hz, 2H), 2.293 (t, 7.575 Hz, 2H), 1.6 (m, 4H), 1.243 (m, 22H). <sup>13</sup>C NMR (CDCl<sub>3</sub>):  $\delta$  174.379, 63.065, 54.434, 34.103, 32.793, 29–24. MS: [M]<sup>+</sup> = 287.4 m/z. Anal. Calcd for C<sub>17</sub>H<sub>34</sub>O<sub>3</sub>: C, 71.28; H, 11.96. Found: C, 71.23; H, 12.13.

**Methyl 16-Fluorohexadecanoate.** Methyl 16-hydroxyhexadecanoate (5.29 g,  $1.85 \times 10^{-2}$  mol) was dissolved in anhydrous methylene chloride (dried over calcium hydride and vacuum-distilled prior to use) in an oven-dried flask under nitrogen. DAST (2.42 mL, 2.97 g,  $1.85 \times 10^{-2}$  mol) was added to anhydrous methylene chloride in a separate oven-dried three-neck flask under nitrogen and charged with a stir bar. The DAST solution was chilled in a dry ice/2-propanol bath, and the methyl 16-hydroxyhexadecanoate solution was slowly cannulated into the

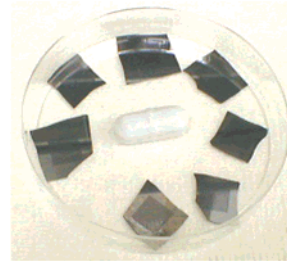


**Figure 2.** The wafers patterned with hydrogels were arranged at the edges of a Petri dish such that a stir bar positioned in the center would not come into contact with them while stirring.

flask while stirring. After 10 min, the solution was warmed to 0 °C to dissolve the frozen methyl 16-hydroxyhexadecanoate and allowed to warm to room temperature while stirring overnight. The solution was transferred to a separatory funnel, and then ether (80 mL) and water (100 mL) were added. The organic layer was isolated, washed with water ( $3 \times 100$  mL), brine ( $2 \times 100$  mL), and saturated NaHCO<sub>3</sub>(aq) ( $2 \times 100$  mL). The organic layer was dried over MgSO<sub>4</sub> and concentrated via rotary evaporation to produce a yellow oil, which solidified at room temperature. The product was purified by column chromatography (19:1 hexane/ethyl acetate), yielding 3.25 g (61%) of the white product. Mp 38–39 °C. <sup>1</sup>H NMR (CDCl<sub>3</sub>):  $\delta$  4.435 (dt, 47.39, 6.25 Hz, 2H), 3.665 (s, 3H), 2.30 (t, 7.525 Hz, 2H), 1.661 (m, 4H), 1.387 (m, 2H), 1.253 (m, 22H). <sup>13</sup>C NMR (CDCl<sub>3</sub>):  $\delta$  174.340, 84.913, 83.611, 51.424, 34.100, 30.491, 29–24. <sup>19</sup>F NMR (CDCl<sub>3</sub>):  $\delta$  –5.887 (tt). MS: [M]<sup>+</sup> = 288.3 m/z.

**16-Fluorohexadecanoic Acid.** Methanol (57 mL), dioxane (90 mL), water (3 mL), and NaOH (7.0 g, 0.175 mol) were added to methyl 16-fluorohexadecanoate (5.271 g,  $1.828 \times 10^{-2}$  mol). The solution was refluxed while stirring overnight (14 h). After cooling to room temperature, the solution formed a gel. Upon neutralizing with excess HCl (25 vol %, 255 mL), a white precipitate in aqueous solution materialized, which was stirred in an ice bath for 1 h. The precipitate was collected and dissolved in ether. The organic solution was dried over MgSO<sub>4</sub>, filtered, and concentrated via rotary evaporation. Recrystallization from hexane yielded 4.16 g (83%) of 16-fluorohexadecanoic acid as white flaky crystals. Mp 74–76 °C. <sup>1</sup>H NMR (CDCl<sub>3</sub>):  $\delta$  4.435 (dt, 47.31 Hz, 6.23 Hz, 2H), 2.346 (t, 7.585 Hz, 2H), 1.67 (m, 4H), 1.255 (m, 24H). <sup>13</sup>C NMR (CDCl<sub>3</sub>):  $\delta$  180.119, 85.074, 83.437, 34.040, 30.498, 30.3–24. <sup>19</sup>F NMR (CDCl<sub>3</sub>):  $\delta$  –5.877 (tt, 24.01 Hz). MS: [M]<sup>+</sup> = 274.2 m/z. Anal. Calcd for C<sub>16</sub>H<sub>31</sub>O<sub>2</sub>: C, 70.03; H, 11.39; F, 6.92. Found: C, 70.06; H, 11.56; F, 6.30  $\pm$  0.36.

**16-Fluorohexadecanoyl Chloride.** Anhydrous benzene (dried over sodium and distilled prior to use) was cannulated into an oven-dried 250-mL three-neck round-bottom flask charged with 16-fluorohexadecanoic acid (2.2766 g, 8.3012 mmol) and a stir bar. Oxalyl chloride (0.72 mL, 1.05 g, 8.30 mmol) was slowly added to the flask, and the solution was stirred at room temperature for 1 h, followed by 6 h in a 60 °C oil bath. The solution was cooled, concentrated via rotary evaporation, and dried in vacuo overnight. The yellow oil was distilled under reduced pressure to yield 2.15 g (89%) of the desired lipophilic acid chloride as a clear liquid. Bp 125 °C/120 mTorr. The product was immediately used for the next reaction.

**Modification of Planar Hydrogel Substrates.** *Synthesis of Fluorinated Fatty Acid Coating.* The procedure employed to modify the planar hydrogel substrates with a fluorinated fatty acid coating was derived from our previously reported procedure for the in situ modification of cylindrical hydrogels within microfluidic devices.<sup>10</sup> The wafer pieces patterned with hydrogel films were arranged within a Petri dish at the outer edges such that a stir bar could be placed at the center without coming into contact with the wafers while spinning (Figure 2). Under atmospheric conditions, a modification solution that consisted of 16-fluorohexadecanoyl chloride (0.58 g, 2 mmol), DMAP (0.024 g, 0.2 mmol), and NEt<sub>3</sub> (0.28 mL, 0.20 g, 2 mmol) in benzene (19.6 mL) was added to the Petri dish, completely submersing the hydrogel substrates. The solution was slowly stirred to simulate the flow of the modification solution through a micro-channel. After 9 h, the samples were removed from the solution,

(13) Sudholter, E. J. R.; van der Wal, P. D.; Skowronska-Ptasinska, M.; van den Berg, A.; Bergveld, P.; Reinhoudt, D. N. *Anal. Chim. Acta* **1990**, *230*, 59–65.

(14) Sheppard, J. N. F.; Lesho, M. J.; McNally, P.; Francomacaro, A. S. *Sens. Actuators, B* **1995**, *28*, 95–102.

(15) Lesho, M. J.; Sheppard, N. F. J. *Sens. Actuators, B* **1996**, *37*, 61–66.

(16) van den Berg, A.; Grisel, A.; Verney-Norberg, E. *Sens. Actuators, B* **1991**, *4*, 235–238.

(17) Revzin, A.; Russell, R. J.; Yadavalli, V. K.; Koh, W.; Deister, C.; Hile, D. D.; Mellott, M. B.; Pishko, M. V. *Langmuir* **2001**, *17*, 5440–5447.

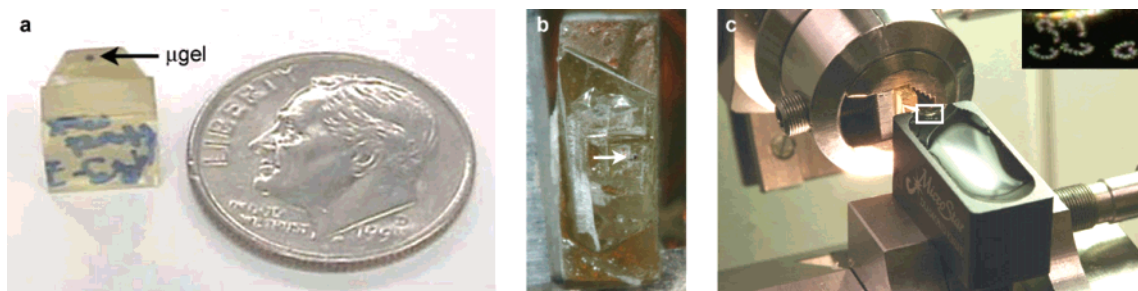


**Figure 3.** Preparation of the embedded sample for TEM. (a) Resin block after repositioning the sample. (b) The block was trimmed with a razor blade so that a small trapezoid of resin that contained a portion of the  $\mu$ gel periphery (white arrow) remained. (c) Using an ultramicrotome, this area was sectioned into thin slices (300 nm) that formed ribbons in the surface of the water within the boat of the diamond knife. The inset is an enlarged image of the area within the white box, depicting ribbons that are formed by multiple thin sections. Each section contains a cross section of the  $\mu$ gel periphery.

washed with methylene chloride to remove excess unreacted reagents, and dried in air.

**Synthesis of Negative Control.** The wafer pieces patterned with hydrogel were arranged within a Petri dish at the outer edges such that a stir bar could be placed at the center without coming into contact with the wafers while spinning. A modification solution that consisted of 16-fluorohexadecanoic acid (0.55 g, 2 mmol) in benzene (19.6 mL) was added to the Petri dish, completely submersing the hydrogel substrates. After 9 h with gentle stirring, the samples were removed from the solution, washed with methylene chloride to remove excess unreacted reagents, and dried in air.

**Surface Characterization of the Modified Hydrogel Substrates.** XPS. XPS was performed on a Physical Electronics PHI 5400 X-ray photoelectron spectrometer using a monochromatic Al X-ray excitation source. Survey scans were performed at 0–1000 eV with a takeoff angle of 45°, and the elemental composition was determined from the survey spectra.

**SIMS.** Samples were sputtered with a thin coat of gold prior to SIMS analysis to minimize sample charging. SIMS was performed on a Cameca ims 5f secondary ion mass spectrometer (Courbevoie, France) employing a 14.5 keV Cs<sup>+</sup> ion source. Negative secondary ions were detected.

**Preparation of Neutral  $\mu$ gels and Characterization with TEM.** *Preparation of Neutral  $\mu$ gels.* The colloidal gold solution used to label the samples for TEM imaging (vide infra) triggered the unwanted expansion of pH-sensitive  $\mu$ gels during sample sectioning. Therefore, all  $\mu$ gels intended for TEM imaging were made from a prepolymer mixture of HEMA with EGDMA (1 wt %) and DMPA (3 wt %). The photopolymerization of the  $\mu$ gel structures within microchannels was performed as described previously.

*Incorporation of the Colloidal Gold Label to  $\mu$ gels.* To label the  $\mu$ gel surface, each channel containing a  $\mu$ gel was filled with an aqueous solution of colloidal gold (20-nm diameter, concentration 0.01% as HAuCl<sub>4</sub> suspended in 0.01% tannic acid with 0.04% trisodium citrate, 0.026 mM potassium carbonate, and 0.02% sodium azide; Sigma). After 2 days, the channel was rinsed with water and acetone to remove the excess gold and dried under N<sub>2</sub> for an additional 2 days.

*Surface Modification of Neutral  $\mu$ gels with Oleoyl Chloride.* Modification of the  $\mu$ gels with oleoyl chloride was performed using a slightly amended version of the procedure reported previously for modification with palmitoyl chloride. For each  $\mu$ gel, a 20-mL syringe was charged to maximum capacity (ca. 25 mL) with 0.1 M oleoyl chloride, 0.1 M NEt<sub>3</sub>, and 0.01 M DMAP dissolved in benzene. As previously described, the filtered solution was flowed through the channel at a high rate until it reached the waste container, then the pump was reprogrammed to a rate of 5 mL/h. When the syringe was empty (ca. 4.5 h), the channel was flushed with methylene chloride to remove precipitate, the needle and tubing were replaced, and a new syringe was charged with fresh solution. The pump was restarted so the solution in the second syringe would flow through the channel in the direction opposite to that previously employed. Up to six  $\mu$ gels were simultaneously modified with this method using the multitrack syringe pump detailed previously.

*Neutral  $\mu$ gel Fixation and Embedment in Resin.* The oleoyl chloride-modified  $\mu$ gels and unmodified  $\mu$ gels (negative controls) were carefully removed from the channels and placed into separate vials. An OsO<sub>4</sub> solution (1% aqueous) prepared from a more concentrated commercially available OsO<sub>4</sub> solution (4%, aqueous) was added to each vial. After 4 h, the OsO<sub>4</sub> solution was removed and the vial was filled with water (20 min). To prepare the samples for embedment in resin, the  $\mu$ gels were dehydrated by replacing the water with a graded series of aqueous ethanol (EtOH) solutions (37% EtOH, 20 min; 67% EtOH, 20 min; 95% EtOH, 20 min; 100% EtOH, 3 times, 30 min each), followed by EtOH/propylene oxide solutions (1:1, overnight; 1:1, 30 min; 10% propylene oxide, 2 times, 1 h each). For the facilitation of resin infiltration, the  $\mu$ gels were then soaked in propylene oxide/Araldite 502 resin (1:1, 1 h), followed by 100% resin (overnight). Each  $\mu$ gel was transferred to a separate cavity of a PELCO 105 flat embedding mold (Ted Pella, Inc., Redding, CA), and the cavity was filled with fresh Araldite 502 resin. The resin was cured in a 60 °C oven for 24 h.

*Sample Reorientation and Sectioning.* The region of the resulting epoxy block that contained the  $\mu$ gel was cut with a rotary tool and glued to the remaining resin block such that sectioning on the microtome would produce radial cross sections of the  $\mu$ gel (Figure 3a). The resin block was trimmed with a razor blade (Figure 3b), and the region of the block that contained the periphery of the  $\mu$ gel was cut into thin sections (300 nm) with a diamond knife (Micro Star Technologies) on a Leica Ultracut UCT ultramicrotome (Figure 3c). The resulting sections were collected on nickel grids (400 mesh, thin bar).

*TEM.* Imaging was performed on a Philips CM200 transmission electron microscope at 120 kV.

## Results

Characterization of the fatty acid-coated  $\mu$ gels started with an investigation of the morphology of the hydrogel surface. A  $\mu$ gel that was modified with palmitoyl chloride was removed from the channel, sputtered with a thin conductive metal coating, and imaged with SEM (Figure 4). The tops and bottoms of the  $\mu$ gels that were in direct contact with the glass channels were fairly smooth and slightly wider than the middle portion of the cylinder. The rounded surface of the  $\mu$ gel cylinder, which was exposed to the modification solution during coating formation, was more irregular and significantly rougher. Ridges and indentations that receded a few micrometers toward the interior of the  $\mu$ gel were clearly visible in this region, signifying these structures would not be amenable to examination with many surface characterization techniques. It is noteworthy that unmodified  $\mu$ gels displayed the same morphology (images not shown), indicating these features were intrinsic to either the  $\mu$ gel photopolymerization process or dehydration but not a result of the modification procedure.

Chemical analysis of the functional groups on the surface of the modified hydrogels was performed with XPS

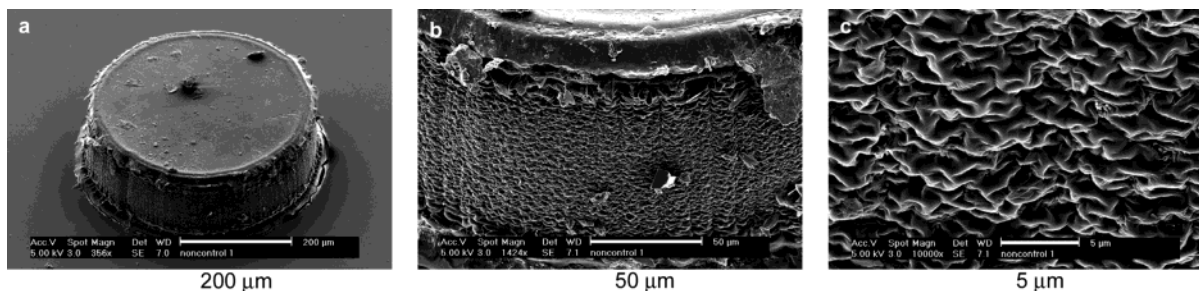
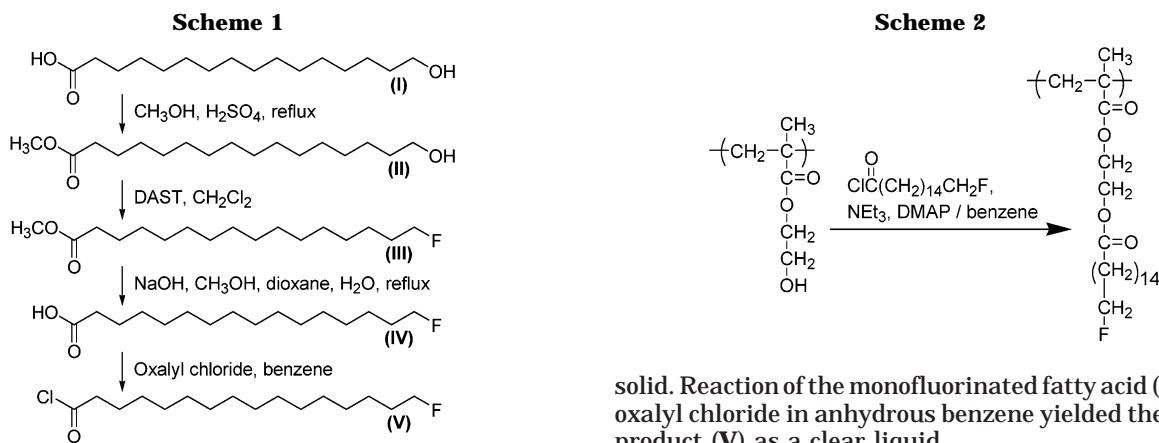


**Figure 4.** A  $\mu$ gel was removed from a microchannel and examined with SEM. (a) The top of the  $\mu$ gel was smooth as a result of contact with the glass microchannel, (b) but the surface exposed to the contents of the channel was very rough. (c) Higher magnification of the side of the  $\mu$ gel that revealed many ridges were present. Debris from the channel was visible on the surface of the  $\mu$ gel.



and SIMS. With these techniques, Ratner et al. confirmed the formation of self-assembled monolayers on polymeric samples by monitoring signals indicative of the resultant urethane linkage.<sup>18</sup> Unfortunately, a similar detection scheme was not applicable to our system because coating fabrication did not form a unique chemical functionality: ester bonds linked the fatty acids to the hydrogel substrate and were already present in the hydrogel matrix. Therefore, a fluorine substituent that served as a chemical probe for the coating was introduced to the lipophilic acid chlorides. In addition to this chemical modification, planar hydrogel substrates were required for analysis with the XPS and SIMS instruments. Hydrogel films on silicon wafers were selected as the planar substrates to minimize the effects of surface charging, which often plagues XPS and SIMS experiments performed on insulating samples.

Thin planar hydrogel substrates of the same chemical composition as the  $\mu$ gels were photopatterned on silicon wafers following previously reported procedures.<sup>13–16</sup> Unlike the  $\mu$ gels in microchannels, SEM imaging revealed these films to be smooth on the micrometer scale (images not shown). To prepare the fatty acid coating, a monofluorinated lipophilic acid chloride was selected instead of a perfluorinated analogue because the monofluorinated compound was chemically more similar to the lipophilic acid chloride that we routinely used for in situ  $\mu$ gel modification. Specifically, an analogue of palmitoyl chloride that contained a terminal fluorine substituent was synthesized from commercially available 16-hydroxyhexadecanoic acid (Scheme 1, **I**). The carboxylic acid functionality was masked as the methyl ester (**II**), followed by conversion of the terminal hydroxyl to a fluoro group with DAST under anhydrous conditions (**III**). Deprotection of the carboxylic acid with base-catalyzed hydrolysis afforded 16-fluorohexadecanoic acid (**IV**) as a crystalline

solid. Reaction of the monofluorinated fatty acid (**IV**) with oxalyl chloride in anhydrous benzene yielded the desired product (**V**) as a clear liquid.

To modify the planar hydrogel substrates with fluorinated fatty acid coatings, a procedure similar to the in situ  $\mu$ gel modification was employed for comparative purposes (Scheme 2). Wafers patterned with thin hydrogel films were submerged in a reaction solution that contained the monofluorinated analogue (**V**) in place of palmitoyl chloride. The solution was gently stirred to mimic laminar flow within microchannels. Negative controls were made in the same fashion, except the modification solution consisted only of 16-fluorohexadecanoic acid (**IV**) dissolved in benzene, which cannot react with the hydrogel substrate under these conditions.

Typical XPS spectra of modified (experimental) and unmodified (negative control) planar hydrogel substrates are shown in Figure 5. The experimental sample clearly displayed a significant fluorine signal (Figure 5a), verifying the presence of the fatty acid coating. In contrast, a strong fluorine signal was absent for the sample treated with monofluorinated fatty acids (negative control, Figure 5b). Because the carboxylic acid moiety of the monofluorinated fatty acid is unlikely to form a covalent linkage to the hydrogel substrate, the absence of a fluorine signal indicates physical absorption was not a sufficient mechanism for coating formation. Corroboration that a coating formed only on the experimental sample was also evidenced by the differences in the carbon and oxygen peak amplitudes between the two specimens. Because XPS probes only the outermost surface (ca. 50–80 Å) of a sample,<sup>19</sup> ester bond formation between the monofluorinated fatty acid chlorides and the hydrogel substrate was expected to increase the carbon peak amplitude and decrease the oxygen peak amplitude relative to the negative control, as was observed.

SIMS was also performed on experimental and control samples. As in the XPS investigation, the presence of a

(18) Kwok, C. S.; Mourad, P. D.; Crum, L. A.; Ratner, B. D. *Biomacromolecules* **2000**, *1*, 139–148.

(19) Briggs, D.; Seah, M. P. *Practical Surface Analysis: Auger and X-ray Photoelectron Spectroscopy*, 2nd ed.; John Wiley & Sons: Chichester, 1992; Vol. 1.

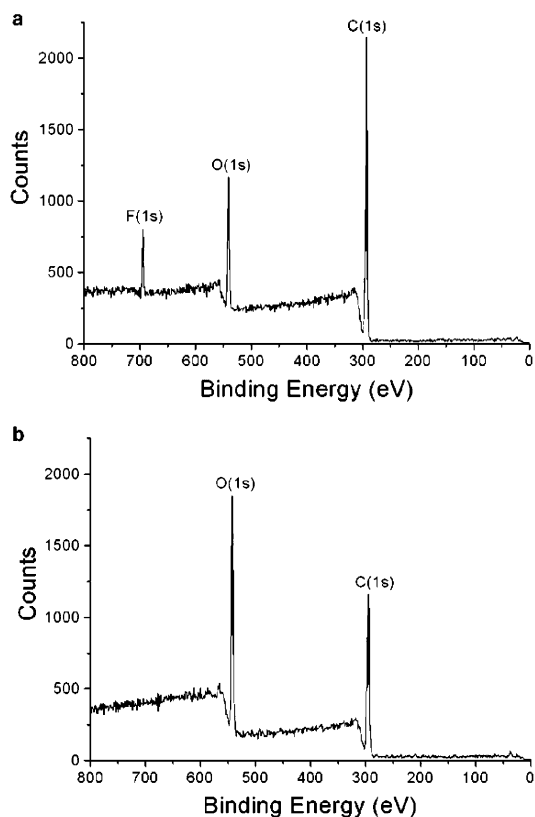


**Figure 5.** XPS spectra of planar hydrogels patterned on wafers. (a) The hydrogel substrate was derivatized with monofluorinated fatty acid chlorides, confirmed by the presence of fluorine. (b) Fluorine was not detected on hydrogel substrates treated with the corresponding monofluorinated fatty acid (negative control).

fluorine signal was used as an indicator of coating formation. Representative SIMS spectra are shown in Figure 6. For the experimental sample (Figure 6a), the fluorine signal abruptly declined from its initial maximum intensity and the oxygen signal intensity rose modestly after 2000 s of sputtering (ca. 1–5  $\mu\text{m}$ ). (SEM imaging of one crater produced by ion sputtering indicated it was approximately 7- $\mu\text{m}$  deep. Although several craters were present, this depth was believed to correspond to a total sputtering time of 3500 s.) This trend is consistent with that anticipated for a hydrogel substrate derivatized near the surface with monofluorinated fatty acid chains, in which removal of the fluorinated coating via ion sputtering uncovers the more oxygen-abundant hydrogel core. In comparison, the negative control displayed very slight and gradual decreases and increases in the oxygen and carbon signal intensities, respectively, over increasing sputtering duration (Figure 6b). The fluorine signal remained at a background level throughout the experiment, indicating the control sample was relatively homogeneous and devoid of a fatty acid coating.

By analogy to membrane studies of living cells, it seemed fitting to adapt microscopy techniques routinely employed for biological sample characterization to further investigate the structure of our fatty acid-coated  $\mu\text{gels}$ . LSCM provides a simple, nondestructive method to characterize small, fluorescent, three-dimensional objects, so this technique was employed to assess the coating location and continuity on the modified  $\mu\text{gels}$ . Although similar lipid and hydrogel hybrids have been imaged with LSCM through the incorporation of fluorescent lipids,<sup>6,7,20</sup> a protocol employed to examine cell membranes was selected

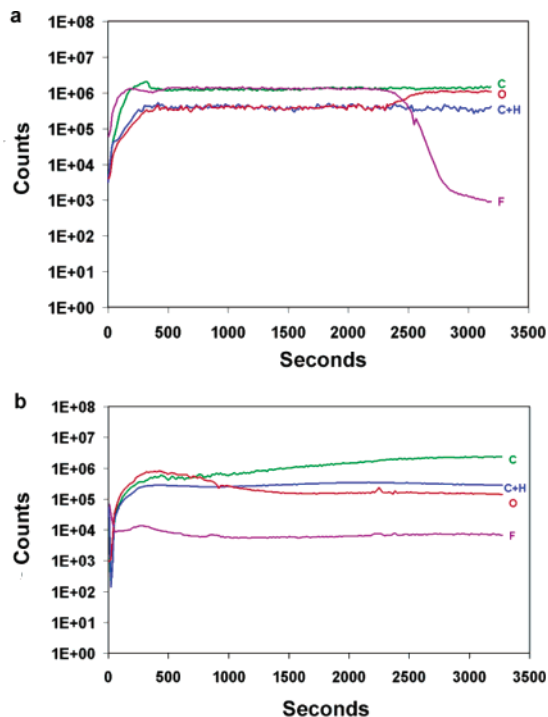


**Figure 6.** SIMS spectra of planar hydrogel samples. (a) The fluorine level abruptly decreased after sputtering the monofluorinated fatty acid chloride-treated hydrogel substrate for 2000 s. (b) The fluorine signal remained at background levels for the monofluorinated fatty acid-treated hydrogel substrate (negative control), indicating a fatty acid coating did not form.

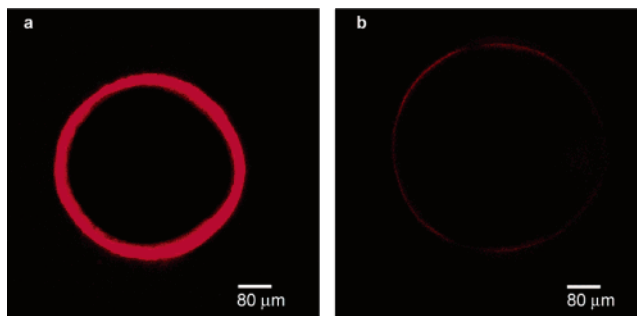
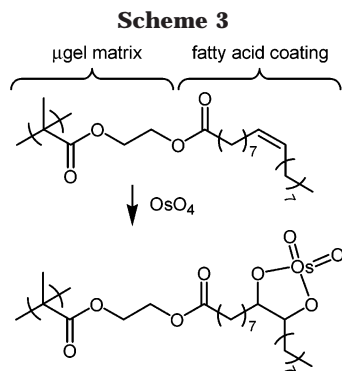


**Figure 7.** Confocal images of a fluorescent lipophilic dye applied to  $\mu\text{gels}$  and imaged in false-color red. (a) The fluorescent signal from the lipophilic dye was present at the periphery of the  $\mu\text{gel}$  modified with palmitoyl chloride, suggesting that the coating was confined within this region. (b) The fluorescent signal from the lipophilic dye was significantly lower for an unmodified  $\mu\text{gel}$  (negative control). The laser power and detector sensitivity employed were identical for direct comparison.

because additional reagents (i.e., fluorescent lipophilic fatty acids) did not need to be incorporated into the in situ modification.<sup>10</sup> The fatty acid coating was visualized while the  $\mu\text{gels}$  were positioned within microfluidic channels by selectively staining the samples with DiD, a lipophilic dye that fluoresces in nonpolar environments such as cell membranes.<sup>21</sup> LSCM imaging revealed strong fluorescence from the lipophilic dye at the periphery of a  $\mu\text{gel}$  modified with palmitoyl chloride using the routine in situ process (Figure 7a). Because DiD selectively partitions into lipophilic environments, the fluorescence signal corresponded to the fatty acid coating, which was thereby

(20) Moya, S.; Donath, E.; Sukhorukov, G. B.; Auch, M.; Baumler, H.; Lichtenfeld, H.; Mohwald, H. *Macromolecules* **2000**, *33*, 4538–4544.

(21) Haugland, R. P. *Handbook of Fluorescent Probes and Research Chemicals*; Molecular Probes, Inc.: Eugene, OR, 1996.



located at the periphery of the  $\mu$ gel. In contrast, significantly less fluorescent signal was detected around unmodified (control)  $\mu$ gels, validating the specificity of the lipophilic dye for the fatty acid coating (Figure 7b). In the modified sample, the selectively stained region was continuous and of constant intensity, but the width varied slightly. Although fluctuations in the laser power and PMT sensitivity considerably affected the observed width of the fluorescent ring making quantitative estimation of the coating thickness from the fluorescent signal unreliable, qualitatively the fatty acid coating appeared to be thicker than a monolayer.

TEM was used to quantitatively measure the depth of the  $\mu$ gel matrix that had been derivatized with fatty acids. Sample preparation for TEM imaging combined protocols for the histology specimen<sup>22</sup> and materials characterization,<sup>4,23–27</sup> which involves selective labeling and fixation with osmium tetroxide ( $\text{OsO}_4$ ), embedment in a resin block, and sectioning into semi-electron transparent slices. For compatibility with this process, slight changes in the chemical composition of the  $\mu$ gel matrix and fatty acid coating were required (vide infra). Initially, the  $\mu$ gel surface was labeled with gold nanoparticles to facilitate identification of the  $\mu$ gel periphery by soaking the samples in a commercially available colloidal gold solution prior to modification. Because the gold solution was buffered to stabilize the suspension, nonionic  $\mu$ gels were employed to prevent expansion during incubation, which would complicate sample preparation. The labeled  $\mu$ gels were dehydrated and modified with oleoyl chloride to create an unsaturated fatty acid coating that could be selectively stained and fixed by the double-bond-reactive reagent,  $\text{OsO}_4$  (Scheme 3). Subsequently, the samples were removed from the channels, stained with  $\text{OsO}_4$ , dehydrated, and embedded in resin. After hardening, the resin blocks were trimmed so that sectioning with an ultramicrotome produced radial cross sections of the  $\mu$ gel periphery.

Modified and unmodified  $\mu$ gel sections were imaged with TEM. In the modified sample, three distinct levels of contrast were visible (Figure 8a). Because the image contrast was produced by the selective transmission of electrons through the sample, these contrast levels were identified as regions composed of three materials of differing electron density. On the basis of the discussion

that follows, we assign these regions as the  $\mu$ gel matrix, the resin in which the  $\mu$ gel was embedded, and the region of the sample stained with  $\text{OsO}_4$  (Figure 9a). The darkest region, a band approximately 9000 nm (9  $\mu\text{m}$ ) in width that separated the other two regions, was attributed to the unsaturated fatty acid-modified portion of the  $\mu$ gel matrix. This band was absent in the unmodified sample (Figure 8b). (The resin in the control appears darker than the resin in the modified sample because the instrument adjusts the contrast relative to the electron transmission within each image.) Additionally, the gold nanoparticles that were used to label the  $\mu$ gel's perimeter were visible at the edge of the dark band within the modified sample (Figure 8c), indicating the position of the band was consistent with the location of the fatty acid coating, at the periphery of the  $\mu$ gel. Likewise, the presence of gold nanoparticles between the two regions of different contrast in the unmodified sample (Figures 8d and 9b) signified that this area was also the  $\mu$ gel/resin interface. The absence of a dark band in the unmodified sample demonstrated that  $\text{OsO}_4$  did not stain the  $\mu$ gel matrix. The images obtained for the modified and unmodified samples were reproducible; examination of several modified and unmodified samples produced similar results. Among the modified samples, the width of the selectively stained fatty acid coating was typically 9  $\mu\text{m}$ , but samples that ranged from 7 to 12  $\mu\text{m}$  were found. Although these measurements were performed on dehydrated  $\mu$ gels, the coating thickness of hydrated samples is expected to also be within this range because water uptake by the hydrophobic fatty acid-functionalized  $\mu$ gel matrix is unfavorable. Noteworthy, the thickness of this band did not increase if the samples were exposed to the  $\text{OsO}_4$  stain for longer time intervals, indicating that the entire modified portion had been stained.

## Discussion

A variety of surface characterization and microscopy techniques were employed to determine the structure of fatty acid-modified  $\mu$ gels synthesized within microfluidic devices for controlled-release or sensory applications. Using these techniques, examination of model systems and the actual hydrogel objects indicated that the hydrogel substrates were functionalized with fatty acids. Modification of the  $\mu$ gel matrix was limited to the perimeter of the sample, and the thickness of this region was on the order of micrometers, as suggested by LSCM and verified with TEM.

Throughout this study, an assumption was made that the planar model systems accurately represented the modified  $\mu$ gels intended for microfluidic applications. Because the validity of the assumption weighs heavily on whether the structural information acquired in this study is applicable to the modified  $\mu$ gels, focus is placed on this issue in the following discussion.

Planar model systems were examined by XPS and SIMS to verify that the reaction conditions employed covalently grafted a fatty acid coating to the hydrogel substrate. The planar hydrogel substrates embodied the chemical composition of  $\mu$ gels photopolymerized within microchannels, albeit the geometry of the hydrogel was altered for these experiments. Modification of the planar system differed from the in situ process in two aspects. First, the reaction solution was slowly stirred for the planar substrates during modification instead of flowing the reagents through microchannels. In both procedures, turbulent mixing within the modification solutions was minimal, so it is unlikely that this difference would significantly influence

(22) Hayat, M. A. *Principles and Techniques of Electron Microscopy: Biological Applications*, 2nd ed.; University Park Press: Baltimore, 1981; Vol. 1, pp 149–210.

(23) Senshu, K.; Yamashita, S.; Ito, M.; Hirao, A.; Nakahama, S. *Langmuir* **1995**, *11*, 2293–2300.

(24) Senshu, K.; Yamashita, S.; Mori, H.; Ito, M.; Hirao, A.; Nakahama, S. *Langmuir* **1999**, *15*, 1754–1762.

(25) Coutandin, J.; Ehlich, D.; Sillescu, H.; Wang, C. *Macromolecules* **1985**, *18*, 589–590.

(26) Mori, H.; Hirao, A.; Nakahama, S. *Macromolecules* **1994**, *27*, 4093–4100.

(27) Kunz, M.; Shull, K. *Polymer* **1993**, *34*, 2427–2430.

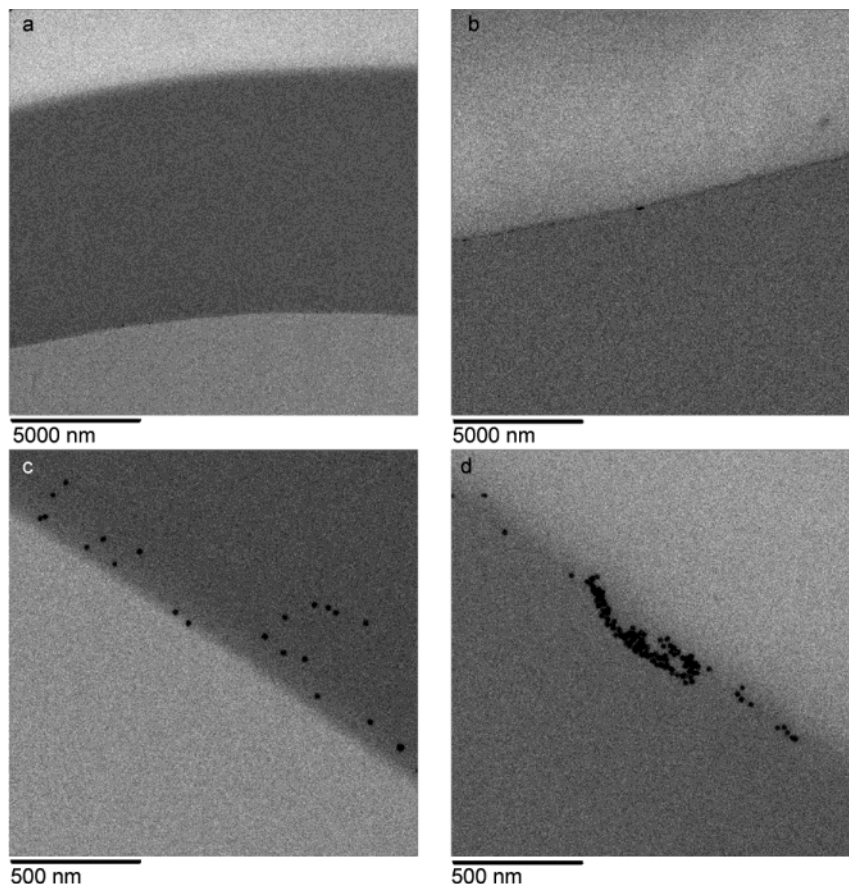


**Figure 8.** TEM images of a sectioned  $\mu$ gel embedded in resin. (a) The  $\text{OsO}_4$ -labeled fatty acid coating appeared as a dark band. (b) Unmodified control samples did not display a dark band, and the visible contrast was due to the difference in contrast between the  $\mu$ gel matrix and the resin in which the sample was embedded. (c) A higher magnification image of the lower edge of the dark band in Figure 8a revealed the gold nanoparticles at the gel/resin interface. (d) Higher magnification of the gel/resin interface of the unmodified control in Figure 8b also revealed that the gold nanoparticles were present.

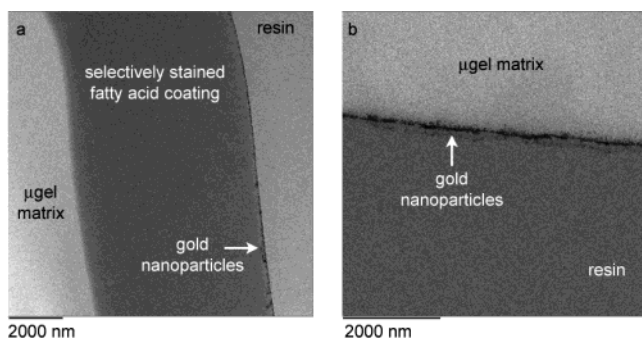


**Figure 9.** Identification of the various regions of contrast in the TEM images of modified and unmodified  $\mu$ gels. (a) The perimeter of the  $\mu$ gel is clearly demarked by gold nanoparticles, which facilitated identifying the modified portion of the  $\mu$ gel that was stained by  $\text{OsO}_4$ . (b) In the unmodified sample, the resin of the embedded sample appears dark relative to the  $\mu$ gel as a result of a difference in the density of the two materials. The gold nanoparticles make the interface unmistakable.

the outcome of the reaction. Second, detection of the coating with XPS and SIMS necessitated substitution of the alkyl fatty acid chlorides with monofluorinated analogues. Though under certain circumstances the more electronegative fluorine substituent can alter the reactivity of the carbonyl functionality to favor coating formation, inductive effects are only operative over short distances,<sup>28</sup> negating this possibility. Overall, these changes bear little

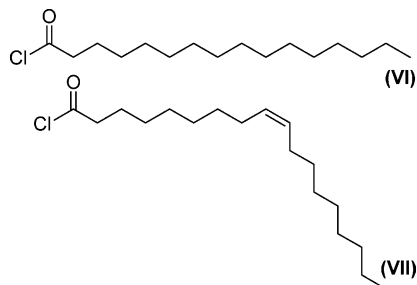
influence on the reactivity of the modification solution, and it is very unlikely that coating formation occurred for the planar model system but not the in situ process. Therefore, this experiment indicated that the reaction conditions employed for the in situ modification procedure covalently attaches a fatty acid coating to the  $\mu$ gels situated within microfluidic devices.

The presence of a fatty acid coating was substantiated by the LSCM investigation, which also demonstrated that the coating was hydrophobic and located at the periphery of the sample. Because LSCM imaging was performed directly on the  $\mu$ gel objects while they were positioned in the microfluidic channels, these deductions are directly applicable to the structure of the modified  $\mu$ gels of interest. LSCM was the only technique that could be performed without altering the composition of the hydrogel objects, but unfortunately it does not have sufficient resolution to pinpoint the depth that the  $\mu$ gel matrix had been derivatized with fatty acids.

The samples studied with TEM were very similar, but not identical, to those created for microfluidic applications. The first difference was that the  $\mu$ gels examined with TEM were not pH-sensitive, which slightly increased the concentration of hydroxyl groups in the  $\mu$ gel matrix. The second dissimilarity relates to the nature of the lipophilic acid chlorides attached to the hydrogel substrate. The samples we envisioned for microfluidic applications are routinely modified with palmitoyl chloride (**VI**), a saturated acid chloride composed of 16 carbon atoms. In comparison, the  $\mu$ gels examined with TEM were treated

(28) Carey, F. A.; Sunberg, R. J. *Advanced Organic Chemistry Part A: Structure and Mechanisms*, 3rd ed.; Plenum Press: New York, 1990.

with oleoyl chloride (VII), an unsaturated analogue composed of 18 carbons.



The influence of these disparities on the thickness of the region derivatized with lipophilic segments is difficult to ascertain. Preliminary studies strongly suggest that this difference in chain length produces negligible variations in the thickness of the  $\mu$ gel's perimeter functionalized with fatty acids. However, cis-unsaturated fatty acid chlorides may produce a fatty acid-derivatized region that is slightly thicker than that produced with the trans-unsaturated isomer.<sup>29</sup> Whether the omission of AA from the  $\mu$ gel matrix significantly alters the thickness of the functionalized sample has not been explored, but the slight increase in the hydroxyl group concentration may negate the influence of the cis double bond. Nevertheless, it is unlikely that these differences in the composition of the modified  $\mu$ gel samples produced a variation in the coating thickness that was greater than the range observed for the samples examined with TEM in this study. Consequently, the thickness of the pH-sensitive  $\mu$ gel's perimeter

functionalized by palmitoyl chloride most likely covers a range centered on 9  $\mu$ m.

### Conclusion

The structure of the fatty acid-modified  $\mu$ gels created within microfluidic devices for controlled-release or sensory applications was elucidated using direct imaging and spectroscopic characterization methods on modified hydrogel structures. The presence of the fatty acid coating was verified by examination of planar model systems with XPS and SIMS. LSCM and the use of a lipophilic fluorescent dye confirmed that the coating was mainly confined to the periphery of the modified  $\mu$ gel. Finally, a TEM investigation that employed samples similar to those integrated into microfluidic devices indicated that the thickness of the  $\mu$ gel's perimeter functionalized with fatty acids was on the order of several micrometers. Through supplementary TEM investigations of the coating thickness produced under different reaction conditions, it may be possible to tailor the permeability characteristics of these objects for specific sensory or controlled-release tasks.

**Acknowledgment.** XPS and SIMS were carried out in the Center for Microanalysis of Materials, University of Illinois, which is partially supported by the U.S. Department of Energy under Grant DEFG02-91-ER45439. Sample sectioning with the ultramicrotome, TEM, SEM, and LSCM imaging were conducted in the Microscopy Suite of the Imaging Technology Group at the Beckman Institute for Advanced Technology, University of Illinois. This work was supported by the National Science Foundation (NSF DMR 01-06608).

(29) Kraft, M. L.; Moore, J. S. Manuscript in preparation.